J. Membrane Biol. 146, 239–251 (1995)

The Journal of
Membrane
Biology


# The Ion Channel Behavior of the Nuclear Pore Complex

**J.O. Bustamante**[1,3], **J.A. Hanover**[2], **A. Liepins**[3]

[1]University of Maryland School of Medicine, Department of Physiology, Baltimore, MD 21201
[2]Laboratory of Biochemistry and Metabolism, National Institute of Diabetes and Digestive and Kidney Diseases, National Institutes of Health, Bethesda, MD 20892
[3]Memorial University of Newfoundland, School of Medicine, Division of Basic Medical Sciences, St. John's, Newfoundland, Canada A1B 3V6

Received: 30 August 1994/Revised: 19 April 1995

**Abstract.** Macromolecule-conducting pores have been recently recognized as a distinct class of ion channels. The poor role of macromolecules as electrical charge carriers can be used to detect their movement along electrolyte-filled pores. Because of their negligible contribution to electrical ion currents, translocating macromolecules reduce the net conductivity of the medium inside the pore, thus decreasing the measured pore ion conductance. In the extreme case, a large translocating macromolecule can interrupt ion flow along the pore lumen, reflected as a negligible pore conductance. Therefore, ion conductance serves as a measurement of macromolecular transport, with lesser values indicating greater macromolecular translocation (in size and/or number). Such is the principle of operation of the widely used Coulter counter, an instrument for counting and sizing particles. It has long been known that macromolecules translocate across the central channel of nuclear pore complexes (NPCs). Recently, large conductance ion channel activity (100–1000 pS) was recorded from the nuclear envelope (NE) of various preparations and it was suggested that NPCs may be the source of this activity. Despite its significance to understanding the regulation of transcription, replication, mRNA export, and thus gene expression of normal and pathological states, no report has appeared demonstrating that this channel activity corresponds to ion flow along the central channel of the NPC. Here we present such a demonstration in adult mouse cardiac myocyte nuclei. In agreement with concepts introduced for macromolecule-conducting channels, our patch clamp experiments showed that ion conductance is reduced, and thus that ion flow is restricted during translocation of macromolecules containing nuclear targeting signals. Ion flow was blocked by mAb414, a monoclonal antibody raised against a major NPC glycoprotein and known to localize on the NPC channel where it blocks macromolecular transport. These results also establish patch clamp as a useful technique for the measurement of macromolecular translocation along the large central channel of the NPC and provide a basis for the design of future investigations of nuclear signaling for control of gene activity, mRNA export for gene expression, as well as other processes subservient to NPC-mediated nucleocytoplasmic exchange.

**Key words:** Nuclear pore complex — Nuclear ion channels — Gene activity — Control of gene expression — Patch clamp — Cardiac myocytes — Cell nucleus

## Introduction

Electron microscopy (EM) studies show that NPCs have a large central channel of roughly 10 nm diameter and 100 nm length (*reviewed in* Panté & Aebi, 1994). Under the assumption that NPCs are perfect circular cylinders, their predicted single channel ion conductance ($\gamma$) is between 100 and 1000 pS (Paine & Horowitz, 1980; *reviewed in* Bustamante, 1994*b*; Bustamante et al., 1994; *see* Estimate of Maximal Ion Conductance of the NPC Channel in Materials and Methods). Given sufficient time (from minutes to hours), NPCs will allow the translocation of particles with cross section smaller than the sieving NPC diameter and of small molecules (<20–70 kD) depending on cell type and phase; *for reviews see*, e.g., Miller et al., 1991; Nigg et al., 1991). The translocation of larger macromolecules is more complex, requiring nuclear localization signals (NLSs), ATP and

*Correspondence to:* J.O. Bustamante

GTP hydrolysis, molecular chaperons, etc., (e.g., Dingwall & Laskey, 1992; Miller et al., 1991; Nigg et al., 1991; Hanover, 1992).

In apparent contradiction, recent patch clamp studies consistently show large conductance (100–1000 pS) ion channel activity at the NE, indicating that nucleocytoplasmic translocation of monovalent ions is restricted and that it occurs in a manner typical of well-known ion channels (e.g., gap junctional channels, ryanodine receptors, mitochondrial and alamethicin channels, etc.); with the channels showing rapid transitions (0.1–10 msec) between the ion conducting and nonconducting states (open and closed, respectively—*reviewed in* Bustamante, 1994*b*; Bustamante et al., 1994). This apparent contradiction is resolved by two concepts. First, the on-off stochastic nature of the gating mechanism of the NPC channel, typical of ion channels, implies that ion flow along the channel is not continuous. That is, the net macroscopic behavior (e.g., that observed in standard light microscopy experiments) is determined by the average behavior of the NPC population. Second, the concepts developed for macromolecule-conducting channels (e.g., Simon & Blobel, 1991, 1992; Bezrukov et al., 1994) indicate that a macromolecule can play the role of a plug for the NPC channel. As recently explained (Bezrukov et al., 1994), the central idea is analogous to the resistive pulse principle used in Coulter counters and other technologies (e.g., Allen, 1967; Bunville, 1984). Briefly, particles that are poor charge carriers decrease the net ion conductance when they move along an electrolyte-filled tubular structure. The magnitude of this decrease is directly related to the particle size and concentration as predicted by the restricted-diffusion theory (e.g., Bean, 1972; Bunville, 1984; Bezkurov et al., 1994).

Based on the above rationale, we took the approaches presented in this and the following two companion papers (Bustamante et al., 1995*b,c*) to determine whether NPCs are the source of the large conductance ion channel currents recorded from the NE and to explore the general effects of macromolecular translocation on NPC channel conductance. Our patch clamp experiments showed that the single NPC channel ion conductance, $\gamma$, was reduced during translocation of macromolecules containing nuclear targeting signals. Ion flow was minimized by what germ agglutinin (WGA) a wide spectrum macromolecular transport blocker (e.g., Miller et al., 1991; Nigg et al., 1991) and, more importantly, by mAb414, a monoclonal antibody raised against a major NPC glycoprotein and known to localize on the NPC channel where it is thought to block NPC-mediated macromolecular transport (e.g., Davis & Blobel, 1986; Finlay et al., 1987; Akey & Goldfarb, 1989; Davis & Fink, 1990; Starr et al., 1990; Clever et al., 1991; Starr & Hanover, 1991; Wente et al., 1992; Rout & Blobel, 1993). Our experimental results demonstrate that the large conductance ion channel activity results from ion flow along the NPC large central channel. The results also show that the NPC conductance behaves as expected for a macromolecule-conducting channel. Therefore, these investigations indicate that patch clamp is a useful technique for assessing NPC-mediated processes such those related to gene activity regulation and expression.[1]

## Materials and Methods

### Nuclei

The method for the isolation of adult cardiac myocyte nuclei has been described elsewhere (Bustamante, 1993). Briefly, cardiac myocytes were isolated from Swiss-Webster mice (20–22 g) according to a standard retrograde-perfusion technique using a high-Na solution (mM: 150 NaCl, 5 $MgCl_2$, 10 HEPES and 5 KOH, pH 7.3–7.4). The resulting myocyte suspension was then purified by a Percoll gradient and centrifuged. The pellet was placed in a Dounce cell grinder containing an ice-cold, high-K, EGTA solution (mM: 135 KCl, 5 $MgCl_2$, 5 EGTA, 5 HEPES and 17.5 KOH, pH 7.2–7.3). Nuclei were mechanically dispersed in this solution with 4–8 strokes of the loose pestle of the grinder. The nuclear suspension was cleaned from debris by passing it through a nylon filter (20 μm mesh) and then stored at 2–4°C in the high-K, EGTA solution for up to 2 hr. Nuclei devoid of ER remains and displaying sharp, smooth contours (100× microscope objective) were selected for these investigations.

### Chemical Reagents and Other Substances

Salt solutions for the bath/perfusing chamber, for the pipette and for cell and nuclei isolation were prepared from pretested reagents (Molecular Biology Grade, Sigma) in Type I reagent grade water obtained 'on demand' from a water purification system (Milli-$Q^{UF}$-PLUS and 0.22 μm Millistak-GS filter, Millipore). A high-K saline solution (mM: 150 KCl, 5 $MgCl_2$, 10 HEPES, and 4 KOH; pH 7.2–7.3) was used as basic control and for the preparation of substrate-enriched media. Wheat germ agglutinin (WGA, ≈36 kD) and puromycin were obtained from Sigma. Two synthetic analogues of the NLS for the SV40 large T antigen were tested: Cys-Gly-Tyr-Gly-Pro-Lys-Lys-Lys-Arg-Lys-Val-Gly-Gly and Pro-Lys-Lys-Lys-Arg-Lys-Val-Glu-Asp-Pro-Tyr-Cys (Sigma). Reticulocyte lysate (TnT) and recombinant activator protein 1 (AP-1, c-Jun, 40 kD) were obtained from Promega. Monoclonal antibody mAb414 (150 kD, isotype IgG1,κ) was used in ascite fluid and protein A-purified (BAbCO, Richmond, CA). In the purified form, mAb414 appeared as a single protein band on SDS-PAGE (BAbCO). Purified mouse IgG1,κ isotype control (Sigma) was used as negative control. The calculated pipette concentration of both mAb414 and its isotype control was ≈70 nM.

[1] It seems necessary to clarify the terminology of channel used in this and the following two companion papers (Bustamante et al., 1995*b,c*). In ion channel theory, a channel is a protein complex with a pore in the center. In nucleocytoplasmic transport theory, the nuclear pore complex is a supramolecular structure with a central, hollow channel (the pore) through which ion and macromolecular translocation occurs. In this and the companion papers we use the second convention when we refer to the NPC channel.

## Patch Clamp

Procedures for patch-clamping isolated nuclei were as previously described (Bustamante, 1992, 1993, 1994*a*). We used fiber-filled glass tubing to pull the patch clamp pipettes (World Precision Instruments). In some tests the pipette was double-filled (e.g., Auerbach, 1991; Ruknudin et al., 1993) with equal amounts (e.g., 4 μl) of the control high-K saline and the test solution (e.g., reticulocyte lysate, WGA, mAb414). This procedure aimed at obtaining a few records of nominal control ion channel activity prior to the onset of action of the test solution. Since some substances may act at subnanomolar concentrations (*see* companion papers, Bustamante et al., 1995*b,c*), both turbulence during double-filling and the glass fiber inside the pipette countered the separation between the control and test solution. However, gentle suction (<10 mm Hg) during gigaseal formation probably drew a few picoliters of the bath control solution into the pipette tip. Independent control experiments (with high-K solution only) in this and previous work (e.g., Bustamante, 1992, 1993, 1994*a*) provided sufficient information to determine the adequacy of the initial recordings as controls. When the initial records did not provide appropriate or sufficiently long controls, we used the results from experiments with high-K solutions only (*see,* for example, Fig. 2). Previous work in this preparation shows that, under our experimental conditions (i.e., high-K solution), the cardiac myocyte nuclei have negligible resting potentials (*see* Bustamante, 1992). Measurements from 24 nuclei confirmed these negligible values (0.2 ± 1.1 mV, mean ± SD). Hence, in the investigations presented here, the potential difference across the NE ($V$; with respect to cytoplasm) is equal to the negative of the pipette potential. All the experiments were carried out in nucleus-attached patches at 22–24°C.

## Ion Conductance

NE permeation was assessed with patch ion conductance ($\Gamma$) by dividing the recorded current, $i$, by the electronmotive force ($V - V_e$):

$$\Gamma = i/(V - V_e)$$

where $V_e$ is the equilibrium electrochemical potential for the ions. Stepwise jumps in the current records, $\Delta i$, represented open ↔ close transitions and were used to calculate the ion conductance of single NPC channels, $\gamma$.

$$\gamma = \Delta i/(V - V_e)$$

Single channel conductance, $\gamma$, was calculated from the measured current jumps, $\Delta i$, and the histograms. The $\Delta i$ values were considered before using the histogram peaks because they are more powerful than histograms in revealing subconductance states (buried in the histograms due to their low probability; e.g., Bustamante, 1994*a*). The maximal current recorded from a patch containing $N$ identical channels would be $N$ times the current for a single NPC channel (i.e., $\Gamma = N\gamma$). For the preparation used in our study, $V_e$ is negligible (e.g., Bustamante, 1992, 1993, 1994*a*). $V_e$ corresponds to the value at which the current reverses its direction (the reversal potential, $V_{rev}$). Therefore, patch ion conductance was obtained by dividing the ion current, $i$ (in pA), generated by the amplitude of the negative of the voltage pulse applied to the NE, $V$ (in mV). In an attempt to properly characterize the statistical properties of the channels, a group or ensemble of records was recorded at more than one voltage. Each ensemble was generated by 8 identical consecutive voltage pulses separated by 300 msec. This minimal number of records per ensemble allowed computations of basic properties, prevented contamination by changing characteristics and saved storage space in the computer. Ensemble averages of ion currents, $\langle i(t) \rangle$, were computed to obtain the average behavior of the channel population (representative of macroscopic or whole-nucleus currents). The probability of opening for the channel population in the patch, $P_o$, was calculated from the equation:

$$\langle i \rangle = P_o\, \gamma\, (V - V_{rev}) = N p_o\, \gamma\, V$$

where $P_o$ equals the number of channels in the patch, $N$, times the open probability of a single channel, $p_o$ (i.e., $P_o = Np_o$) and, in our case, $V_{rev} \approx 0$. Hence, $P_o = \langle i \rangle / \Delta i$. The $P_o$ values were normalized to their maximum for comparison with other experiments. We have previously shown that the single channel conductance, $\gamma$, of our preparations is independent of voltage (Bustamante, 1992, 1993). That is, the current-voltage relationship follows a straight line. Therefore, although we tested several values of pipette potential in all the experiments, only patch clamp recordings for one voltage amplitude are given, when sufficient and appropriate, for the sake of clarity. Pulses of opposite polarities were applied because it was found that the NPC antibody blockade could appear at only one polarity of the pulse (unipolar blockade). This unidirectional phenomenon was never observed with unplugged NPC channels in our control condition with high-K solution.

## Estimate of Maximal Ion Conductance of the NPC Channel

The predicted, theoretical maximum of ion conductance for a single NPC channel, $\gamma_{max}$, (i.e., electrolyte-filled channel, absence of nonconducting molecules) was calculated from the published dimensions of the NPC channel in *Xenopus laevis* oocytes (e.g., Panté & Aebi, 1994). Estimates based on NPC geometry have been given elsewhere (e.g., Paine & Horowitz, 1980). In its simplest form, if a channel has radius $r$ and a length $\lambda$, and is filled with a medium of resistivity $\rho$, then:

$$\gamma_{max} = \pi\, r^2\, \rho^{-1}\, \lambda^{-1}$$

The actual conductance of the NPC channel will be the difference between the maximal value of $\gamma$ during ion conduction (i.e., $\gamma_{max}$) and nonconduction modes (*see* Bezkurov et al., 1994, and references therein).

Measurement theory, which uses the instrumentation errors to calculate the error intrinsic to a measurement, indicates that the relative error in the $\gamma_{max}$ estimate equals the sum of the relative errors in each of the component quantities, according to the following equation:

$$\Delta\gamma_{max}/\gamma_{max} = (\Delta\rho/\rho) + 2\,(\Delta r/r) + (\Delta\lambda/\lambda)$$

where the $\Delta$'s represent the errors for each variable. For example, for a channel of 5 nm radius, $r$, and 100 nm length, $\lambda$, one has 20% and 1% error with a microscope of 1 nm resolution. Under the assumption that the relative error in $\rho$ is negligible, the relative error in $\gamma_{max}$ is 41% or 205 pS for a 500 pS channel. Thus, the instrumentation error can be significant and indicate that a small standard deviation (SD)-to-mean ratio (the experimental error) can be deceptive. Therefore, in absence of accurate measurements of NPC dimensions for our preparations, we think that the conductance values recorded in our experiments fall within the predicted range.

## Fluorescence Microscopy

Fluorescence microscopy was carried out in either a custom microscope (Bustamante, 1991, 1993) or in a laser-scanning confocal microscope (MRC-600, BioRad). Nuclei were imaged through a 100× objective. Macromolecular transport along the NPC channel was moni-

tored as previously reported (e.g., Starr et al., 1991). A fluorescent probe using the NPC channel for nuclear localization was prepared as previously described (Wolff et al., 1988). The probe consisted of B-phycoerythrin (240 kD, Molecular Probes) conjugated to a synthetic NLS analog of the SV40 large T antigen (Cys-Gly-Tyr-Gly-Pro-Lys-Lys-Lys-Arg-Lys-Val-Gly-Gly, Sigma). Negative controls were carried out with a probe consisting of B-phycoerythrin conjugated to an NLS-incompetent mutant (Cys-Gly-Tyr-Gly-Pro-Lys-**Thr**-Lys-Arg-Lys-Val-Gly-Gly, mutation in bold type). TRITC-labeled WGA (≈36 kD) was purchased from Sigma.

## Electron Microscopy

Transmission EM was carried out to obtain an estimate of the number of NPCs per unit area and thus, of the number of NPCs under the recording pipette. Nuclei were fixed in glutaraldehyde and post-fixed in osmium tetroxide (Sigma), according to a standard EM procedure (Bustamante et al., 1981, 1982). Estimates were calculated following the procedure previously used for other nuclear preparations (Mazzanti et al., 1991). Briefly, the distance between neighboring NPCs was measured, averaged and squared to obtain the NPC density per unit area. This approach can only be considered a rough estimate because of artifacts intrinsic to EM specimen preparation and known to affect specimen dimensions (for a discussion *see* Mazzanti et al., 1991), although our EM procedure was previously shown to produce little shrinkage of sarcomere length (Bustamante et al., 1981, 1982). From measurement theory the relative error in the area of the square used to estimate NPC surface density is twice the relative error in the distance between neighboring NPCs.

## Theory

The topic of macromolecular translocation through ion channels is relatively unexplored because most ion channels studied do not allow transport of macromolecules. Therefore, a brief review of the highlights of macromolecule-conducting channel concepts, as they apply to NPCs, is given below. Note that in this and the following papers attention is not paid to peripheral channels observed in structural studies (Hinshaw et al., 1992) as this could not be confirmed independently (Akey & Radermacher, 1993; *reviewed* in Bustamante et al., 1994; Panté & Aebi, 1994). Figure 1 illustrates the macromolecule-conducting channel model applied to NPCs. When the NPC channel is occupied by a translocating macromolecule, ion flow along the channel is restricted and may be interrupted if the macromolecule if sufficiently large to plug the channel. When the channel is not occupied by macromolecules, the gates of the channel open and close and ion flow proceeds in a way similar to well-known ion channels. The bottom traces of Fig. 1*A* show actual signals of ion conductance in response to 2 sec pulses from 0 to −10 mV (pipette voltage). When the NPC channels are closed, the ion conductance is negligible whereas when they are open, a sizable ion conductance appears if the channel is not occupied by one or more translocating macromolecules. A brief channel closing is shown to illustrate that more than one channel was present in the patch. Panel *B* of Fig. 1 shows, in qualitative terms, the predicted reduction in $\gamma$ during macromolecular translocation and blockade. Plugging macromolecules should result in open $\leftrightarrow$ close transition times larger than those typical of plasmalemmal ion channels. Therefore, patch clamp should be able to detect long transition times (e.g., >10 msec) during macromolecular entry to and exit from the NPC channel. The transition time from the open to the plugged states and from the plugged to the open (unplugged) states would be determined by the specific characteristics of the interactions between the translocating macromolecule and the cytoplasmic and nucleoplasmic sides of

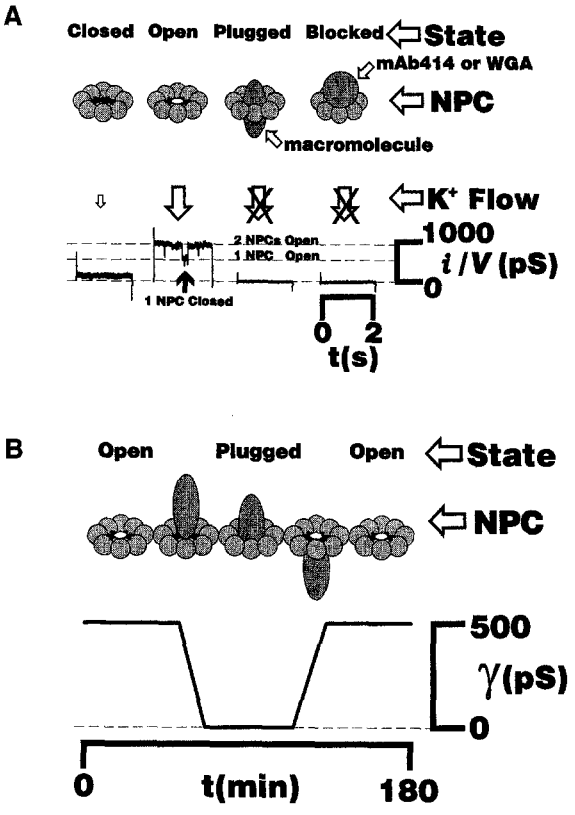


**Fig. 1.** Macromolecule-conducting channel model of NPC-mediated transport. (*A*) Sketch of the effects of macromolecule and small ion translocation on single NPC ion channel conductance, $\gamma$. For simplicity, the NPC is represented by a single ring of eightfold geometry. On-off gating is carried out by an iris-like mechanism responding to nuclear and cytosolic processes. Under the influence of the electrical potential, *V*, electrical charge carriers move along the NPC channel. This movement results in the recorded ion current, *i*. Macromolecules and water are not as good carriers as small physiological ions are. Normal NPCs whose central channel is free from macromolecules are filled with aqueous ionic medium, rich in electrical charge carriers, and display large and small or negligible conductance in the open and close state, respectively. When occupied by large macromolecules, NPCs display a negligible ion conductance. Small molecules only cause a reduction of the conductivity of the medium and, therefore, they do not interrupt but rather reduce ion flow. When the NPC channel is blocked by molecules that dock in the cytoplasmic entrance (e.g., mAb414, WGA) the single ion conductance, $\gamma$, may also be zero. The ion conductance of a single NPC channel is derived from the single ion current jumps, $\Delta i$, according to Ohm's law: $\gamma = \Delta i/V$, Shown on the bottom are actual ion conductance records obtained with 2 sec-pulses from 0 to −10 mV. The second record from the left shows two conductance levels corresponding to the opening of two NPC channels. The single channel conductance for this record is the difference between the two conductance levels (marked with dashed lines). (*B*) Predicted ion conductance behavior according to the model in (*A*). Before macromolecular translocation, the NPC channel is only filled with electrolyte. Therefore, $\gamma$ is maximal. As the macromolecule, a poor electrical charge carrier, lodges into the mouth of the channel, $\gamma$ is reduced according to the degree of obstruction caused by the macromolecule. The kinetics of this phenomenon is determined by the translocation mechanism used by the particle in transit (e.g., whether it requires ATP hydrolysis or whether it interacts with the NPC channel lining). The slopes of conductance, $\gamma$, vs. time, *t*, and the behavior of $\gamma$ during translocation, may be used in quantifying NPC-mediated macromolecular translocation.

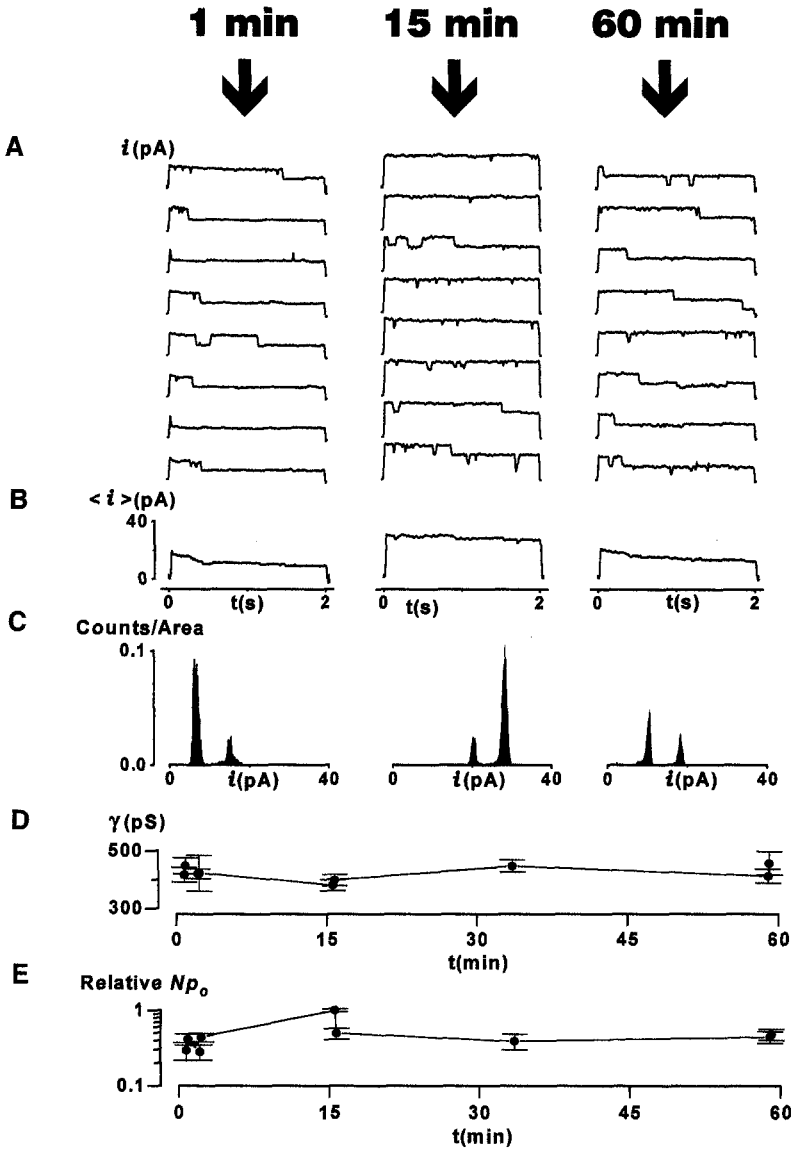


**Fig. 2.** Control patch activity maintained high conductance throughout long-term recordings. (*A*) Ensembles of ion current, $i(t)$, elicited with pipette pulses from 0 to −20 mV. The potential at which the currents reversed direction, $V_{rev}$, was 0 mV. The ensembles shown correspond to 1, 15 and 60 min of patch-clamp recording. The experiment was carried out in control conditions, with high-K saline. (*B*) Averages of the ion current ensembles, $\langle i(t) \rangle$, shown in (*A*). (*C*) Current histograms from the current ensembles in (*A*). The histograms were normalized to the area. (*D*) Time course of single channel conductance, $\gamma$, calculated from current step-transitions, $\Delta i$, detected in the experiment. The data points correspond to the means calculated for each ensemble. Error bars superimposing the filled circles represent the standard deviations. A total of 66 jumps, during pulses from 0 to ±10 and ±20 mV, could be resolved in this experiment. (*E*) Time course of relative open probability, $P_o = Np_o$, calculated from the mean $\langle i \rangle$ and the measured single channel conductance, $\gamma$, where $N$ represents the number of functional channels in the patch and $p_o$ the open probability of a single channel: $\langle i \rangle = Np_o\gamma\,(V - V_{rev})$.

the NPC (e.g., like friction, a stronger interaction would prolong transition times). This may explain the recently reported slow transitions (msec–min) between the conducting and nonconducting states of NE ion channels (NICs, Bustamante, 1994*a*; Bustamante et al., 1994). As previously shown (Bustamante, 1992, 1993, 1994*a*; Dale et al., 1994; Mazzanti et al., 1994), the gating mechanism of the NPC channel may display inactivation (i.e., time-dependent decay in opening probability), the cause of which is still not known. Voltage-dependent inactivation would explain the reported increase in NE resistance to ion flow with large nucleocytoplasmic ion concentration gradients (Al-Mohanna et al., 1994).

## Results

### Large Ion Conductance Activity

With saline alone in the pipette, the recorded channel activity had a single ion channel conductance, $\gamma$, of 421 ± 46 pS (mean ± SD, obtained from averages of 451 records, 16 patches, 12 control mice). Our analysis of the stochastic properties of channel activity is shown in Fig. 2. (*See* Colquhoun & Hawkes, 1983). Panel *A* in Fig. 2 gives three ensembles of patch current records, $i(t)$, acquired at 1, 15 and 60 min after gigaseal formation between the pipette and the patched membrane. The discrete, stepwise jumps in the current records, $\Delta i$, indicate open ↔ close transitions of single functional channels of the patch. Figure 2*B* gives the current averages, $\langle i(t) \rangle$, obtained from the ensembles in panel *A*. These averages reveal the inactivating and noninactivating behavior that we previously reported (Bustamante, 1992; *see* also Dale et al., 1994; Mazzanti et al., 1994). Current amplitude histograms were used to calculate the mean values of the current levels. Figure 2*C* shows histograms for the ensembles in Fig. 2*A*. For comparison, the histograms were normalized to unity by dividing the counts over the

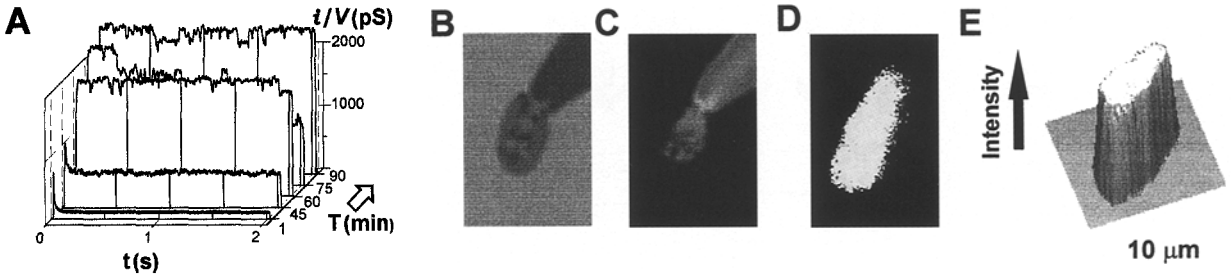


**Fig. 3.** Ion flow is restricted by macromolecular translocation. (*A*) Selected traces of patch ion conductance, *i/V,* following voltage pulses from 0 to +25 mV. The traces demonstrate that the channels were initially plugged by the 240 kD fluorescent probe (B-phycoerythrin conjugated to the NLS of the SV40 large T antigen, 200 nM, *see* Fluorescence Microscopy in Materials and Methods). Thirty minutes later, the channels began to unplug due to the successful translocation of the probe molecules to the nuclear interior. Transport substrates were provided by the reticulocyte lysate. The time of acquisition for each trace is shown on the axis labeled T(min)—counted from the moment the pipette was filled. Prior to attaching the patch-clamp pipette to the NE, the nuclei were washed with high-K saline for 15 min to remove macromolecular transport substrates. (*B*) Standard transmission light microscopy demonstrating the general features of the nucleus-attached patch used in the experiment illustrated in *A*. (*C*) Epifluorescence microscope image of the preparation in *A* and *B*. Only after 30 min was the fluorescence microscope image intense enough for detection. This is due to the small area through which macromolecular transport took place (pipette tip diameter about 1.5 μm). (*D*) Fluorescence microscope image demonstrating the macromolecular transport capacity of the nuclei used in the present study. The image was taken after 15-min treatment with the reticulocyte lysate containing the nuclear targeted B-phycoerythrin, followed by washout with high-K saline to eliminate background fluorescence. (*E*) Three-dimensional rendering of fluorescence image in *D*.

area of the unprocessed plot. In the experiment of Fig. 2, no subconductance states were detected. Panel *D* in Fig. 2 shows the time course of the single channel conductance, $\gamma$, calculated from the $\Delta i$ values for different times during the experiment. The mean $\gamma$ throughout the experiment was 423 ± 25 pS (mean ± SD, 66 jumps). The time course of relative $P_o$ for the experiment illustrated in Fig. 2 is given in the bottom panel *E*. Note that at 15 min, there is a pronounced increase in relative $P_o$. This increment corresponds to the increased amplitude in the current ensemble shown in panel *A* of Fig. 2 (15 min column) which, in turn, results in the larger ensemble average of panel *B*. This direct relationship between the magnitude of the patch current (and thus, the corresponding conductance, $\Gamma = i/V$) and the open probability of the patch, $P_o$, holds true whenever the conductance of a single channel, $\gamma$, remains constant. EM determinations of NPC surface density gave a rough estimate of 12 ± 4 NPC.$\mu m^{-2}$ (mean ± SD, $n$ = 32, 2 mice, *see* Electron Microscopy in Materials and Methods). This estimate confirmed the presence of NPCs in our NE patches (1–2 μm pipette tip diameter) but suggests that several NPC channels must have not been operational (*see* Discussion).

### Translocation of Nuclear Targeted B-Phycoerythrin Opposes Ion Flow

The selected patch ion conductance, *i/V,* traces of Fig. 3*A* illustrate 1 of 10 experiments carried out with reticulocyte lysate containing the nuclear-targeted fluorescent probe (B-phycoerytrin conjugated to the NLS of SV40 large T antigen, *see* Fluorescence Microscopy in Materials and Methods). In these experiments, only the patch clamp pipette contained the lysate. The traces show that the B-phycoerytrin molecules (240 kD, 100 nM), plugged the NPC channel in less than 30 sec but completely translocated to the nuclear interior after 30 min (10 out of 10 experiments), thus clearing and making the NPC channels ready for ion flow (final $\gamma$ = 452 ± 84 pS). This interpretation was supported by simultaneous and independent fluorescence microscopy observations as shown in Fig. 3*B* and *C* and 2*D* and *E,* respectively (10 mice, 220 nuclei, 10 of which were imaged simultaneously to patch clamp recordings). That is, detection of nuclear internalization of the probe was simultaneous to the appearance of ion channel openings (100% of tests), indicating that macromolecular translocation countered ion flow across NPCs. This time-dependent increase in patch conductance reflected the increase in relative $P_o$ from 0 (at 0 min) to 1 (at 90 min), with a time to half value of 47 ± 9 min ($n$ = 10). To confirm that nuclear import of the probe did not result from an abnormally permeable NE, we used a probe consisting of B-phycoerythrin conjugated to a localization-incompetent, single-point mutant of the NLS from the SV40 large T antigen (6 patches, one mouse per patch, *see* Fluorescence Microscopy in Materials and Methods). Neither nuclear import of the probe nor a change in NIC activity were observed (100% of tests; $\gamma$ = 415 ± 74 pS). These results are independent confirmation that the NE was not damaged in our preparation.

### Wheat Germ Agglutinin Blocks Ion Flow

We tested the effects of WGA on both ion channel activity and macromolecular transport (12 patches, 6 mice).

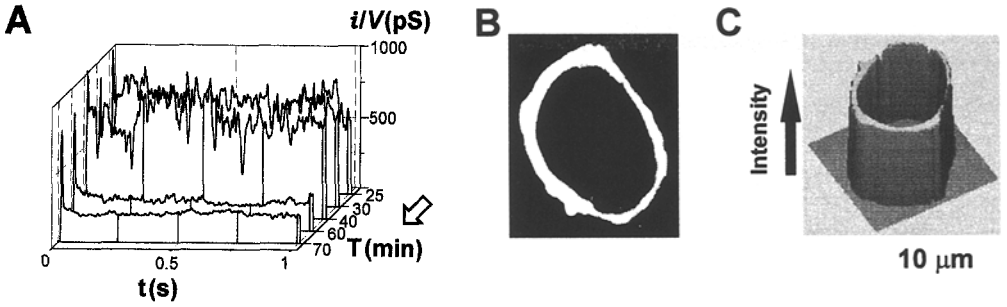


**Fig. 4.** NPC ion channel behavior is blocked by wheat germ agglutinin, WGA. (*A*) Selected traces of patch ion conductance, *i/V*, elicited with pulses from 0 to –40 mV. The acquisition time for each trace is indicated in the axis labeled T(min). The first 4 mm length of the pipette tip was filled with high-K saline and another 4 mm length was filled with the same plus 250 μM of the lectin. (*B*) WGA localizes on the NE and blocks macromolecular transport. Fluorescent microscope image demonstrating localization of TRITC-labeled WGA on the NE and blockade of macromolecular transport by the lectin. The nucleus was exposed for 5 min to 250 μM of the lectin, then 200 nM of the B-phycoerythrin probe was added for 30 min, and then washed with the high-K saline to eliminate background fluorescence. (*C*) Three-dimensional rendering of the fluorescence intensity image in *B*.

Figure 4 illustrates the actions of WGA. The recordings of Fig. 4*A* show that WGA caused a decrease in patch ion conductance, Γ, whereas the fluorescence microscopy of Fig. 4*B* and *C* demonstrates that WGA localized on the NE and prevented macromolecular transport as expected (e.g., Miller et al., 1991; Nigg et al., 1991). These results were consistent in all the 12 tested patches, with changes in single ion channel conductance, γ, from 398 ± 86 to 60 ± 43 pS, at 0 and >50 min, respectively. The lower value at the end of the experiments suggests partial blockade of the channel. The corresponding change in relative $P_o$ went from 1 at the start of the experiments (0 min) to 0.4 ± 0.1 at the end (>50 min), when the effect of WGA had reached its maximum. Note that the apparently high values at the end of the experiment are the result of a lower single channel conductance.

### Ion Channel Activity Derives from the Nuclear Envelope

Since the endoplasmic reticulum (ER) is continuous with the outer membrane of the NE, it may be argued that NICs are related to the protein-conducting channels of the ER (Simon & Blobel, 1991, 1992). We tested the possibility that the recorded channel activity derived from the ER channels by adding 1–100 μM puromycin, a known opener of these channels (Simon & Blobel, 1991), to the pipette solution and the bath (22 patches with saline alone and 6 patches with reticulocyte lysate, 5 mice). In contrast to observations with ER channels (Simon & Blobel, 1991), puromycin failed to modify ion channel activity in all patches (10 at 1 μM, 4 of which were with lysate; 8 at 10 μM, 2 with lysate; and 4 at 100 μM, 2 with lysate; γ = 426 ± 47 pS—*not shown*). Eight additional tests with 100 μM puromycin in silent patches (i.e., no ion channel activity, γ = 0 pS; presumably having all NPCs plugged with macromolecules), with saline alone produced no effect (*not shown*). These results confirm that the ion channel activity recorded from the NE did not derive from the ER channels. Localization signals open the protein-conducting channels of the ER (Simon & Blobel, 1992). Therefore, we also tested two synthetic analogues of the NLS for the SV40 large T antigen (*see* Materials and Methods). The two NLSs failed to open or modify NIC activity (100% of 12 patches, 6 mice—*not shown*).

### mAb414 Blocks Ion Flow

The results presented so far provide evidence that NIC activity may be associated with NPCs. To unequivocally establish that NIC activity derives from NPCs we hypothesized that a monoclonal antibody raised against a major NPC glycoprotein, known to localize on NPCs channel and to block macromolecular transport, may be more specific than WGA in interfering or blocking ion translocation along the NPC channel. Therefore, we selected the monoclonal antibody mAb414 (IgG1,κ isotype), which fulfills these conditions (e.g., Davis & Blobel, 1986; Finlay et al., 1987; Akey & Goldfarb, 1989; Davis & Fink, 1990; Starr et al., 1990). Figure 5 shows records from one of the screening experiments with ascite fluid containing mAb414 (≈70 nM, 11 patches, 3 mice). The results, observed in all tested patches, were consistent with the hypothesis that the recorded NIC currents correspond to ion flow along the NPC channel. However, to exclude the possibility that undetermined contaminants in the ascite fluid may have caused these effects, we furthered these studies with protein A-purified mAb414 (≈70 nM, 22 patches, 19 mice). Figure 6 illustrates two experiments displaying the two modes of action observed with purified mAb414: bi- and unipolar blockade. We include our observation of unipolar blockade (2 patches) because it demonstrates that mAb414

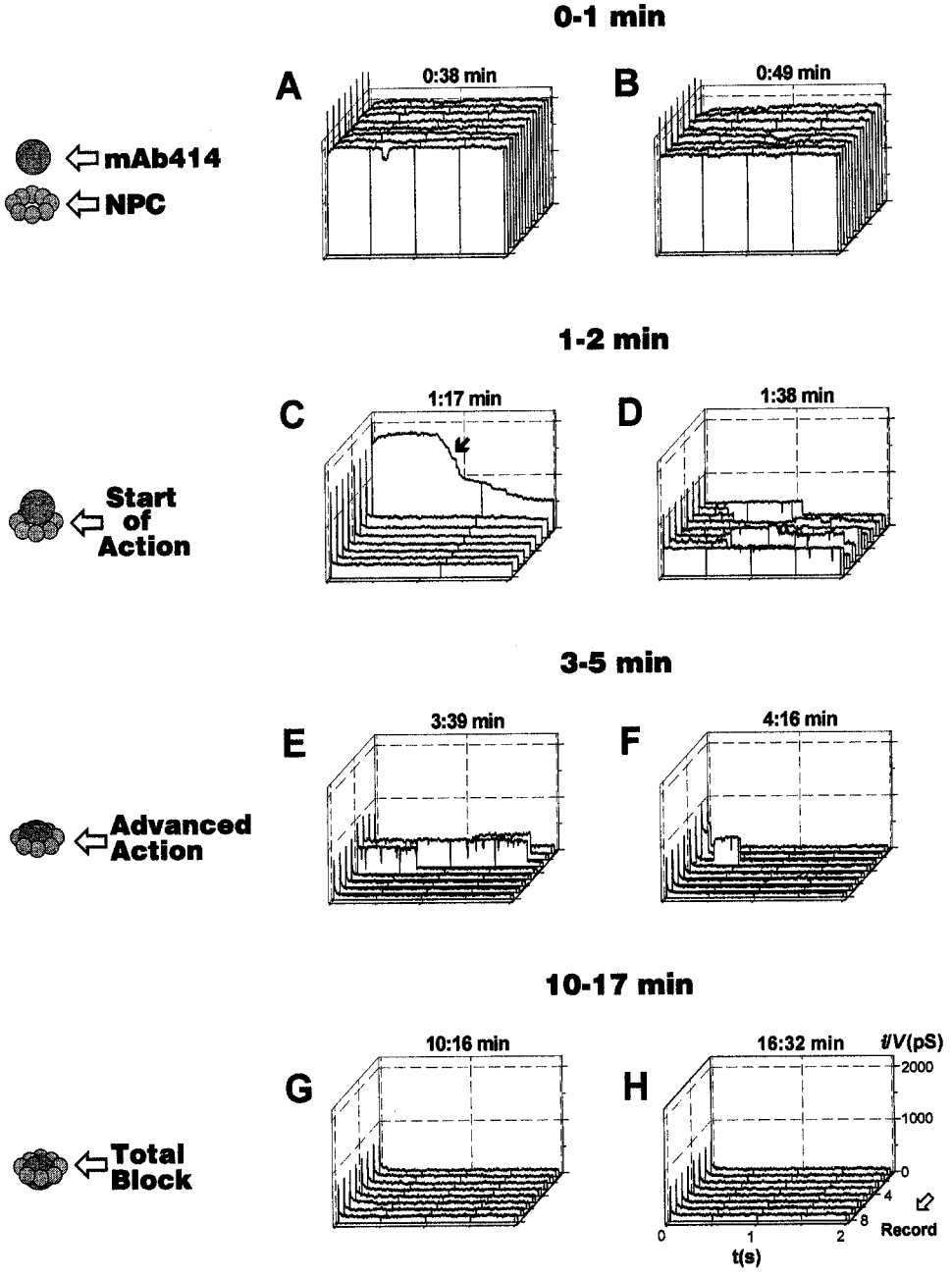


**Fig. 5.** mAb414, a monoclonal antibody against a major NPC glycoprotein blocks ion channel activity. (*A–H*) Ensembles of patch ion conductance records elicited at 300 msec interval with voltage pulses from 0 to −25 and +25 mV (left and right panels, respectively). Opposite pulse polarities are illustrated because two experiments showed a polarity-dependent blockade (*see* Fig. 6). The time of acquisition of each ensemble is shown on top of each panel. Calibration for all panels is shown in panel H. The interpretation of the course of events according to the macromolecule-conducting channel model is shown on the left column of the figure. (*A–B*) Control ion channel activity. Initial activity of the patch channel population showing their maximal activation as indicated by the maximal number of ion-conducting channels. (*C*) Start of blocking action by mAb414 (ascite fluid, 70 nM). Initial reduction in the number of ion-conducting channels is indicated by the downward arrow pointing to the first trace in the ensemble. (*D–H*) Continued decrease in number of functional channels was demonstrated by the increment in the number of records showing no channel opening.

action is not the result of macromolecular plugging (*see* Fig. 1). That the effect was intrinsic to the antibody action of mAb414 was confirmed by the lack of action of a mouse IgG1,κ isotype control (≈70 nM, 30-min recordings, 6 patches, 6 mice). As mAb414 action resulted in total block (in one or two directions), no single channel opening was observed. Since during unidirectional blockade no change in single channel conductance was

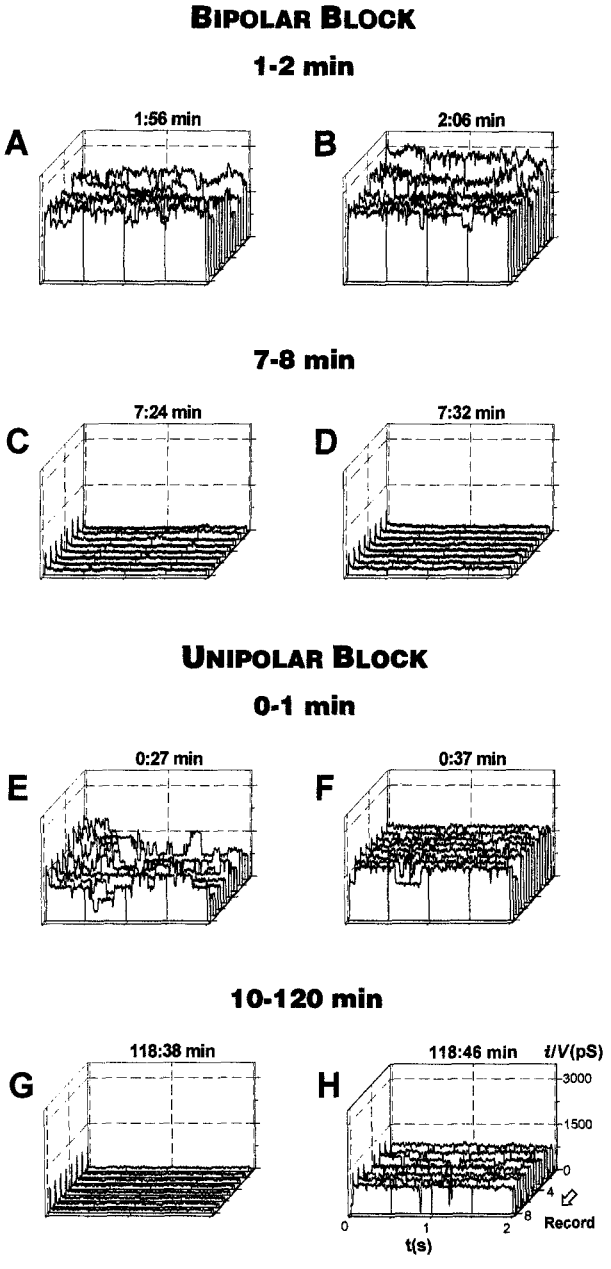


**Fig. 6.** The two modes of blockade action of mAb414: bipolar and unipolar. (*A–H*) Patch conductance ensembles elicited with pulses from 0 to −10 and +10 mV (left and right panels, respectively). The time of acquisition of each ensemble is shown on top of each panel. Protein A-purified mAb414 was used at 70 nM concentration. Calibration for all panels is shown in panel *H*. (*A–D*) Bipolar block of ion channel activity is indicated by total interruption of ion flow with positive and negative voltage polarities. (*E–H*) Unipolar block for a different patch. Only ion flow in one direction was blocked, a demonstration that blockade is not the result of NPC channel plugging. This phenomenon served to exclude the possibility that the apparent block resulted instead from plugging of the NPC channel by the large mAb414 molecule (≈150 kD). (*A, B*) and (*E, F*) Channel activity at the beginning of the experiments (<2 min) served as reference as no antibody action had taken effect in the antibody-loaded pipette. (*C, D*) and (*G, H*) Block of ion flow by mAb414. Unipolar block (*G, H*) developed within 10 min and was followed for 2 hr to confirm that it was not a transient phenomenon.

observed, we concluded that only the cytoplasmic side of the NPC was blocked. Therefore, the changes in relative $P_o$ went from 1 at the beginning of the experiment (0 min), to 0 when mAb414 action took effect (7 ± 2 min).

### Translocation of Natural Karyophilic Protein Transiently Interrupts Ion Flow

These results provide substantial evidence that the large conductance NIC activity corresponds to ion flow along the NPC channel. To test whether or not the macromolecule-conducting channel paradigm is correct we used a native nucleophilic macromolecule known to bind to DNA and to exclusively use the NPC channel for its nuclear translocation: the proto-oncogene product known as activator protein 1 (AP-1, 40 kD). Figure 7 demonstrates that indeed ion channel flow is prevented during macromolecular translocation of the protein molecule along the NPC channel (1 pM, 6 patches, 1 mouse per experiment, 3–6 hr recordings). Single channel conductance before and after the effect of AP-1 (at 1:17 min, Fig. 7*B*) was 330 ± 28 pS. Relative $P_o$ changed from 0.48 at the start to the maximum of 1.00 at end of the experiment (0 and 150 min, respectively). The experiments in this series consistently showed no change in single channel conductance. They all showed plugging of the channels at 1–2 min (1.5 ± 0.3 min) and unplugging after 90 min (109 ± 5 min). The initial relative $P_o$ for all the patches was 0.4 ± 0.1.

## Discussion

### Electron Microscopy Indicates that the Recording Patch-Clamp Pipette Contains NPCs

In agreement with previous reports (e.g., Mazzanti et al., 1991), our EM measurements confirmed that the patch clamp pipette contained one or more NPCs. Under the assumption that the computed NPC surface density reflects the true value, then several NPC channels must have not been operating in the ion-conducting mode. That is, some of the channels may have been plugged, blocked and/or permanently closed. We think that this reduced number of functional channels may be an indication that some NPC channels had been plugged by translocating macromolecules, thus stopping ion flow and avoiding patch clamp detection. The fact that we did not add ATP during nuclei isolation may explain this phenomenon (*reviewed in* Panté & Aebi, 1994). An additional factor is one that is common to all ion channels. Since all NPC channels in a patch appear to operate independently (Bustamante, 1992), they need not open at the same time. Channel opening is a stochastic process whose probability depends on various process such as

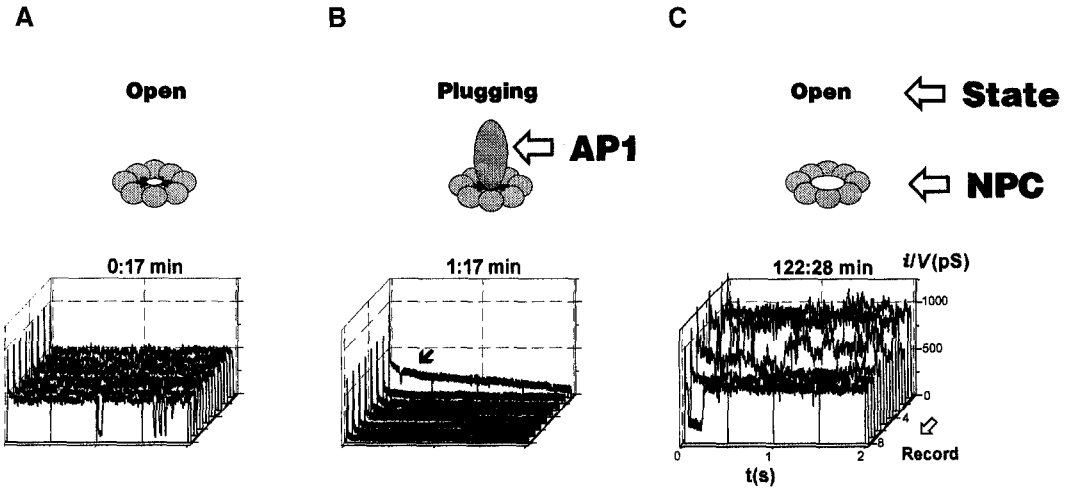


**Fig. 7.** Translocation of natural nuclear protein restricts ion flow. (*A–C*) Records of patch ion conductance elicited with pulses from 0 to −10 mV. Calibration for all panels is shown in panel *C*. Interpretation of the phenomenon according to the macromolecule-conducting channel model is illustrated on top of each panel. (*A*) NPC ion channel behavior prior to macromolecular entrance of activator protein 1, AP-1 (c-Jun, 40 kD). Only one NPC was functioning as a typical ion channel: with stochastic openings and closings. Therefore, patch ion conductance reflected the activity of a single NPC. (*B*) Plugging of the NPC channel by the protein. Decline of ion flow upon presentation of the c-Jun molecule to the mouth of the channel (first record in the ensemble pointed by the arrow). This initial phase of decline, lasting only about 2 sec, was followed by a 2 hr impairment of ion flow. (*C*) Restoration of NPC ion channel activity after completion of macromolecular translocation. Note that two NPCs, instead of one as in *A*, were operating as ion channels.

protein phosphorylation/dephosphorylation and G-protein-mediated mechanisms (e.g., Bustamante, 1992, 1994*b*; Bustamante et al., 1994). However, experiments such as that shown in Fig. 7 points to the first possibility: that of plugged channels. If indeed several NPCs were plugged during isolation, then this phenomenon may be exploited in the future to assess single NPC channel function by reducing the number of functional channels.

### The Recorded Ion Conductance of a Single Channel Falls within Theoretical Range

The recorded activity had a single ion channel conductance, $\gamma$, of 421 ± 46 pS ($n$ = 451). This value agrees with that previously reported for this preparation (Bustamante, 1992, 1993) and is within the range predicted for a cylinder of published NPC dimensions (100–1000 pS, *see* Estimate of Maximal Ion Conductance of the NPC Channel in Materials and Methods). Structural studies of cardiac myocyte NPCs are unavailable. Therefore, our estimates were based on general NPC dimensions provided in the EM literature (*see* Panté & Aebi, 1994). Preliminary investigations with field emission scanning EM (≈1 nm-resolution; Bustamante et al., *in preparation*) indicate that in our cardiac myocytes, the NPCs are not uniformly distributed as is the case for *Xenopus laevis* oocytes (e.g., Goldberg & Allen, 1993). Furthermore, cardiomyocyte NPCs do not show constant diameter. This observation is similar to that made for *Xenopus l.* (*see,* e.g., Figs. 3*B,* 4*E* and 8*E–H* in Golberg & Allen, 1993). Consequently, variabilities in measured $\gamma$ should be expected even for the same NE.

### Translocation of Nuclear Targeted B-Phycoerythrin Opposes Ion Flow

Since patch clamp studies of NE ion channels, NICs, have been carried out in saline solutions devoid of substrates for macromolecular transport, the argument may be raised that the recorded ion channel activity does not correspond to ion flow along the NPC channel because macromolecular transport studies suggest that NPCs do not open in saline solution alone (e.g., Adam et al., 1990, 1991; *discussed in* Bustamante, 1994*b*; Bustamante et al., 1994). This argument is an extension of that given in the first paragraph of our Discussion, except that the hypothesis is raised here that all the NPC channels could have been artificially closed or plugged, so that the source for the recorded channel activity had no relation to NPCs. Our patch clamp measurements of monoatomic ion flow (e.g., Fig. 2; *see also* Bustamante, 1992) as well as our fluorescent microscopy observations of B-phycoerythrin translocation (e.g., Fig. 3) demonstrate that cardiac myocyte nuclei were capable of macromolecular transport and that ion channel activity was silent during periods attributed to macromolecular translocation. It is possible that the movement of the probe from the pipette to the nucleus (e.g., Fig. 3*C*) could have been

artificially produced by an increase in membrane tension associated with the pipette-NE interactions. That this was not the case was demonstrated by the nuclear localization of the probe in whole nuclei (e.g., Fig. 3*D*). An important conclusion may be reached from these observations. The very reticulocyte lysate, which is widely used for its content of substrates for macromolecular transport (e.g., Adam et al., 1990, 1991) actually antagonizes NPC ion channel behavior because it contains macromolecules capable of translocating through, and plugging the channel. Such macromolecules include transcription factors (*discussed in the following companion papers:* Bustamante et al., 1995*b,c*), and heat shock cognate proteins, which act as chaperons in nucleocytoplasmic transport (e.g., Dingwall & Laskey, 1992) and shuttle between nucleus and cytoplasm (e.g., Mandell & Feldherr, 1990; Lin et al., 1994). That is, the exposure to reticulocyte lysate should be expected to result in an initial plugging of the NPC channel followed by clearance and, therefore, manifest itself as a transient (1–5 hr) reduction of ion flow through the NPC channel.

### Ion Channel Activity in the Presence of Agents Known to Interact with NPCs

WGA, ≈36 kD, a lectin known to block macromolecular transport by binding to glycoprotein sites inside the NPC channel (e.g., Miller et al., 1991), reduced ion channel activity (both conductance, $\gamma$, and opening probability, $P_o$) and prevented nuclear import of the nuclear-targeted B-phycoerytrin (e.g., Fig. 4), suggesting that the ion channel activity was related to NPCs. Since recent experiments show that 40 kD dextran molecules translocate readily through cardiac myocytes NPC channels (*see* Bustamante et al., 1995*b*), the WGA-induced reduction in channel conductance must have resulted from the known binding of WGA molecules to the NPC channel interior, for otherwise the WGA molecules would have translocated to the nuclear compartment. The failure of puromycin to open the NE ion channels excluded the possibility that these channels were the protein-conducting channels of the ER (Simon & Blobel, 1991, 1992). Failure of signal peptides, NLSs, to cause ion channel activity in either high-K saline alone or in the presence of reticulocyte lysate also indicates that, at difference from ER protein-conducting channels, the NPC channel is not opened by NLSs alone.

The monoclonal antibody mAb414 (IgG1,$\kappa$ isotype), raised against a major NPC protein, is known to localize inside the lumen of the NPC channel and to block macromolecular transport (e.g., Davis & Blobel, 1986; Finlay et al., 1987; Akey & Goldfarb, 1989; Davis & Fink, 1990; Starr et al., 1990; Clever et al., 1991; Starr & Hanover, 1991; Wente et al., 1992; Rout & Blobel, 1993). Blockade of ion channel activity by mAb414 proves that the recorded ion current corresponds to ion flow along the NPC channel. This conclusion is supported by the lack of action of the mAb414 isotype control. However, it may be argued that the mAb414 molecules may have acted as plugs rather than blockers. This argument was disproved by our fortuitous observation of unipolar blockade in 2 (out of 22) patches. That is, mAb414 caused blockade of ion flow in one direction only. We think that this type of blockade resulted from loose binding of the mAb414 molecule which rendered it susceptible to voltage polarity due to exposure of mAb414 charged residues. Our results with mAb414 (bipolar or total blockade) resemble those obtained for the large $K^+$-conductance $Ca^{2+}$ release channel of the sarcoplasmic reticulum (Chen et al., 1993) and for gap junctional channels (Hertzberg et al., 1985; Hertzberg, 1985).

The experimental results with activator protein 1, AP-1, known to translocate to the nuclear interior exclusively via NPC channels prove that the NPC channel follows the general paradigm for macromolecule-conducting channels (Simon & Blobel, 1991, 1992; Bezkurov et al., 1994). Since the single channel conductance, $\gamma$, was the same before and after the plugging period, the lower value of relative $P_o$ at the start of the experiments suggests that the number of functional channels at the start of the recordings was lower than at the end of the experiments (*see* panels *A* and *C* in Fig. 7). That this phenomenon does correspond to plugging of the channel and not to a prolongation of the closed time or reduction of open time is illustrated by the clear decline in single channel conductance shown in Fig. 7*B*. The decline was relatively fast and could be detected with the 2 sec-records. This indicates that it is feasible to measure with patch clamp such events as signal transduction to the nucleus, mRNA export and proteins using NPCs to shuttle between nucleus and cytoplasm. Further discussion of these observations and their significance are given in the two companion papers describing our investigations with transcription factors NF-$\kappa$B and SP1 and with the TATA-binding protein (TBP, Bustamante et al., 1995*b,c*). Our results with natural karyophilic macromolecules explain why silent nuclear envelope patches are frequently observed when the isolated nuclei are left in cell lysate at room or higher temperatures (Bustamante, *unpublished results*). This observation is consistent with macromolecules translocating and plugging the NPCs, thus giving the misleading impression that the NPCs are artificially closed. Indeed, recent experiments with such silent patches show that after a period of 1–2 hr in saline alone, ion channel activity emerges, consistent with the concept of the macromolecule-conducting channel. That NE conductance increases with ATP was recently reported in elegant studies with *Xenopus I.* oocytes (Mazzanti et al., 1994). The authors interpreted their results as a direct modulation of single NPC chan-

nel conductance by ATP, rather than an direct effect of ATP in the clearing of the channels from plugging macromolecules. That is, no mention was made of the macromolecule-conducting channel theory. We think that in our case, the role of ATP was actually to accelerate the unplugging of the NPC channel by macromolecules, as predicted by nucleocytoplasmic transport theory (e.g., Miller et al., 1991; Nigg et al., 1992; Dingwall & Laskey, 1992).

### Novel View of NPC Function: The Macromolecule-Conducting Channel Model

The present studies demonstrate for the first time that the central channel of the NPC behaves in a manner predicted by the concepts developed for macromolecule-conducting channels (e.g., Simon & Blobel, 1991, 1992; Bezkurov et al., 1994). That is, when the lumen of the channel is occupied by poor electrical charge carriers like nuclear proteins and macromolecular complexes (e.g., mRNA), the effective conductivity of the medium decreases, thus leading to smaller values of single ion channel conductance, $\gamma$. In the extreme case of large macromolecules, the ion flow is interrupted due to plugging of the NPC channel. Like ion channels of other organelles and of the cell surface, NPC channel probability of opening, $p_o$, is regulated by ligands, substrates for hydrolysis of ATP (Mazzanti et al., 1994) and GTP (Bustamante, 1993), second messengers, protein kinases and phosphatases, etc., (Bustamante, 1992). Regulation of monoatomic ion flow can be expressed in terms of NPC ion conductance, $\gamma$, and opening probability, $p_o$. Since macromolecular translocation counters ion flow, it is possible to assess nucleocytoplasmic transport of molecules from changes in $\gamma$, $p_o$, and other NPC ion channel characteristics. Under the macromolecule-conducting channel paradigm, one may interpret the transitions between noninactivating and inactivating channel behavior (*see* Fig. 2 and Bustamante, 1992) in terms of molecules that gain access to the NPC channel mouth and act as a chain-and-ball mechanism, in a manner similar to that of well-known inactivating channels. Taken together, this novel view of NPC function is significant to understanding the role of NPCs as mediators of the signaling mechanisms regulating gene expression. Our work shows the potential of combined patch clamp and microscopy techniques in elucidating the elusive and intricate mechanisms of nucleocytoplasmic exchange and signal transduction to the nucleus (Hofmann, 1993; Marx, 1993).

Thanks are tendered to Dr. W. Jonathan Lederer, University of Maryland at Baltimore, for help with laser scanning confocal fluorescence microscopy and to Dr. Robert A. Prendergast, Johns Hopkins University, for discussion and guidance on the antibody experiments. We are greatly indebted to Joe Sanguedulce, Mike Hernández, and Harrison L. Weese of Nissei Sangyo America, Ltd., for their help with high-resolution, field emission EM. This work was supported by the American Heart Association, Maryland Affiliate, to JOB, National Institutes of health Intramural Funding to JAH, and the Medical Research Council of Canada to AL.

## References

Adam, S.A., Sterne-Marr, R., Gerace, L. 1990. Nuclear protein import in permeabilized mammalian cells requires soluble cytoplasmic factors. *J. Cell Biol.* **111:**807–816

Adam, S.A., Sterne-Marr, R., Gerace, L. 1991. *In vitro* nuclear protein import using permeabilized mammalian cells. *Meth. Cell Biol.* **35:**469–482

Akey, C.W., Goldfarb, D.S. 1989. Protein import through the nuclear pore complex is a multistep process. *J. Cell Biol.* **109:**971–982

Akey, C.W., Radermacher, N. 1993. Architecture of the *Xenopus* nuclear pore complex revealed by three-dimensional cryo-electron microscopy. *J. Cell Biol.* **122:**1–19

Allen, T. 1967. Particle Size Analysis. pp. 110–127. Soc. Anal. Chem. Publ., London

Al-Mohanna, F.A., Caddy, K.W.T., Bolsover, S.R. 1994. The nucleus is insulated from large cytosolic calcium ion changes. *Nature* **367:**745–750

Auerbach, A. 1991. Single channel dose-response studies in single cell-attached patches. *Biophys. J.* **60:**660–670

Bean, C.P. 1972. Membranes. G. Eisenman, editor. pp. 1–54. Dekker, New York

Bezkurov, S.M., Vodyanoy, I., Parsegian, V.A. 1994. Counting polymers moving through a single ion channel. *Nature* **370:**279–281

Bunville, L.G. 1984. Modern Methods of Particle Size Analysis. H.G. Barth, editor. pp. 1–42. Wiley, New York

Bustamante, J.O. 1991. An inexpensive inverted microscope for patch-clamp and other electrophysiological studies at the cellular level. *Pfluegers Arch.* **418:**608–610

Bustamante, J.O. 1992. Nuclear ion channels in cardiac myocytes. *Pfluegers Arch.* **421:**473–485

Bustamante, J.O. 1993. Restricted ion flow at the nuclear envelope of cardiac myocytes. *Biophys. J.* **64:**1735–1749

Bustamante, J.O. 1994*a*. Open states of nuclear envelope ion channels in cardiac myocytes. *J. Membrane Biol.* **138:**77–89

Bustamante, J.O. 1994*b*. Nuclear electrophysiology. *J. Membrane Biol.* **138:**105–112

Bustamante, J.O., Liepins, A., Hanover, J.A. 1994. Nuclear pore complex ion channels. *Mol. Membr. Biol.* **11:**141–150

Bustamante, J.O., Liepins, A., Prendergast, R.A., Hanover, J.A., Oberleithner, H. 1995*c*. Patch-clamp and atomic force microscopy demonstrate TATA-binding protein (TBP) interactions with the nuclear pore complex. *J. Membrane Biol.* **146:**000–000

Bustamante, J.O. Watanabe, T., McDonald, T.F. 1981. Single cells from adult mammalian heart: isolation procedure and preliminary electrophysiological studies. *Can. J. Physiol. Pharmacol.* **59:**907–910

Bustamante, J.O., Watanabe, T., McDonald, T.F. 1982. Non-specific proteases: a new approach to the isolation of adult cardiocytes. *Can. J. Physiol. Pharmacol.* **60:**997–1002

Bustamante, J.O. Oberleithner, H., Hanover, J.A., Liepins, A. 1995*b*. Patch-clamp detection of transcription factor translocation across nuclear pores. *J. Membrane Biol.* **146:**000–000

Chen, S.R.W., Zhang, L., MacLennan, D.H. 1993. Antibodies as probes for $Ca^{2+}$ activation sites in the $Ca^{2+}$ release channel (ryanodine receptor) of rabbit skeletal muscle sarcoplasmic reticulum. *J. Biol. Chem.* **268:**13414–13421

Clever, J., Yamada, M., Kasamatsu, H. 1991. Import of simian virus 40

virions through nuclear pore complexes. *Proc. Natl. Acad. Sci. USA* **88:**7333–7337

Colquhoun, C., Hawkes, A.G. 1983. Principles of stochastic interpretation of ion-channel mechanisms. *In:* Single Channel Recording. Sakmann B. and E. Neher, editors. pp. 135–175. Plenum, New York

Dale, B., DeFelice, L.J., Kyozuka, K., Santella, L., Tosti, E. 1994. Voltage clamp of the nuclear envelope. *Proc. Roy. Soc. London* **255:**119–124

Davis, L.I., Blobel, G. 1986. Identification and characterization of a nuclear pore complex protein. *Cell* **45:**699–709

Davis, L.I., Fink, G.R. 1990. The NUP1 gene encodes an essential component of the yeast nuclear pore complex. *Cell* **61:**965–978

Dingwall, C., Laskey, R. 1992. The nuclear membrane. *Science* **258:**942–947

Goldberg, M.W., Allen, T.D. 1993. The nuclear pore complex: three-dimensional surface structure revealed by field emission, in-lens scanning electron microscopy, with underlying structure uncovered by proteolysis. *J. Cell Sci.* **106:**261–274

Hanover, J.A. 1992. The nuclear pore: at the crossroads. *FASEB J.* **6:**2288–2295

Hinshaw, J.E., Carragher, B.O., Milligan, R.A. 1992. Architecture and design of the nuclear pore complex. *Cell* **69:**1133–1141

Hoffman, M. 1993. The cell's nucleus shapes up. *Science* **259:**1257–1259

Lin, W.Q., Van Dyke, R.A., Marsh, H.M., Trudell, J.R. 1994. Nuclear translocation of heat shock protein 72 in liver cells of halothane-exposed rats. *Biochem. Biophys. Res. Comm.* **199:**647–652

Mandell, R.B., Feldherr, C.M. 1990. Identification of two hsp70-related *Xenopus* oocyte proteins that are capable of recycling across the nuclear envelope. *J. Cell Biol.* **111:**1775–1783

Marx, J. 1993. Forging a path to the nucleus. *Science* **260;**1588–1560

Mazzanti, M., DeFelice, L.J., Cohen, J., Malter, H. 1990. Ion channels in the nuclear envelope. *Nature* **343:**764–767

Mazzanti, M., DeFelice, L.J., Smith, E.F. 1991. Ion channels in murine nuclei during early developments and in fully differentiated adult cells. *J. Membrane Biol.* **121:**189–198

Mazzanti, M., Innocenti, B., Rigatteli, M. 1994. ATP-dependent ionic permeability on nuclear envelope in *in situ* nuclei of *Xenopus* oocytes. *FASEB J.* **8:**231–236

Miller, M., Park, M.K., Hanover, J.A. 1991. Nuclear pore complex: structure, function and regulation. *Physiol. Rev.* **71:**681–686

Nigg, E.A., Baeuerle, P.A., Lührmann, R. 1991. Nuclear import-export: in search of signals and mechanisms. *Cell* **66:**15–22

Paine, P.L., Horowitz, S.B. 1980. The movement of material between nucleus and cytoplasm. *Cell Biol.* **4:**299–338

Panté, N., Aebi, U. 1994. Towards understanding the three-dimensional structure of the nuclear pore complex at the molecular level. *Curr. Opin. Struct. Biol.* **4:**187–196

Rout, M.P., Blobel, G. 1993. Isolation of the yeast nuclear pore complex. *J. Cell Biol.* **123:**771–783

Ruknudin, A., Sachs, F., Bustamante, J.O. 1993. Stretch-activated ion channels in tissue-cultured chick heart. *Am. J. Physiol.* **264:**H960–H972

Schumacher, R.J., Hurst, R., Sullivan, W.P., McMahon, N.J., Toft, D.O., Matts, R.L. 1994. ATP-dependent chaperoning activity of reticulocyte lysate. *J. Biol. Chem.* **269:**9493–9499

Simon, S.M., Blobel, G. 1991. A protein-conducting channel in the endoplasmic reticulum. *Cell* **65:**371–380

Simon, S.M., Blobel, G. 1992. Signal peptides open protein-conducting channels in *E. coli*. *Cell* **69:**677–684

Starr, C.M., D'Onofrio, M., Park, M.K., Hanover, J.A. 1990. Primary sequence and heterologous expression of nuclear pores glycoprotein p62. *J. Cell Biol.* **110:**1861–1871

Starr, C.M., Hanover, J.A. 1991. A common structural motif in nuclear pore proteins (nucleoporins). *BioEssays* **13:**145–146

Wente, S.R., Rout, M.P., Blobel, G. 1992. A new family of yeast nuclear pore complex proteins. *J. Cell Biol.* **119:**705–723

Wolff, B., Dickson, R.B., Hanover, J.A. 1988. Nuclear protein import: specificity for transport across the nuclear pore. *Exp. Cell Res.* **178:**318–334